ELSEVIER

Materials Science and Engineering B101 (2003) 77–88

MATERIALS SCIENCE & ENGINEERING B

www.elsevier.com/locate/mseb

Controlling the quantum dot nucleation site

Nunzio Motta [a,b,*], Anna Sgarlata [b], Federico Rosei [b,c], P.D. Szkutnik [b], S. Nufris [b], M. Scarselli [b], A. Balzarotti [b]

[a] *INFM-Dipartimento di Fisica, Università di Roma TRE, Via della Vasca Navale 84, 00146 Rome, Italy*
[b] *INFM-Dipartimento di Fisica, Università di Roma 'Tor Vergata', Via della Ricerca Scientifica n. 1, 00133 Rome, Italy*
[c] *INRS-EMT, Université du Québec, 1650 Boul. L. Boulet, Varennes, Quebec, Canada J3X 1S2*

Abstract

Quantum dots (QDs) are actually easily produced by self-assembling during heteroepitaxial growth of semiconductors. In order to exploit the unique electronic properties of semiconductor QDs in novel quantum effect devices, the lateral dimensions of these structures have to be reduced to the order of tens of nanometers, which is the range of the De Broglie wavelength of electrons inside these materials. Moreover, millions of QDs must be arranged in dense ordered arrays to achieve the necessary active volume for optoelectronic applications. Nowadays it is possible to control size and shape of the nanocrystals, but it is still difficult to decide their nucleation site. Many approaches have been undertaken to overcome this problem, like using regular dislocation networks, lithographically and Atomic Force Microscopy (AFM) patterned substrates, naturally patterned surfaces. We present results obtained by some of these methods, visualized by Scanning Tunnelling Microscopy (STM) or AFM microscopy. STM measurements at high temperature during the epitaxial growth are of great help in these studies. Images and movies of the growth of Ge on Si help to identify the real nucleation sites of the islands and to follow their evolution. The influence of the 'step bunching' on the self-organization of Ge islands on Si(111) surfaces will be analysed, as an example of growth on self-nanostructured surfaces.

Keywords: Quantum dots; Nanostructures; Ge/Si; STM; AFM

1. Introduction

The production of coherent crystalline islands of nanometric sizes on semiconducting substrates is actually easily achieved thanks to the deep knowledge of the epitaxial growth which has been reached in recent years. It is well known that the growth of an element with lattice parameter different from that of the substrate gives origin to small islands, relieving the strain between epilayer and substrate. If the crystal lattice of these islands is coherent with the substrate and no dislocation occur, these islands are perfect crystals, with sizes limited to few tens of nanometers. People usually refer to these islands as 'quantum dots' (QD), due to the confinement of electrons in all three dimensions occurring when the structures sizes are in the range of the De Broglie wavelength of electrons inside the chosen material. However, in order to exploit the electronic properties in new quantum effect devices, two main problems have still to be solved: the ordering of these islands on the substrate, and the optimum control of their lateral dimensions. These two problems are actually strongly interconnected, and reaching a perfect control of the lateral ordering should give in turn a better homogeneity in the QD sizes.

Advances in crystal growth techniques such as Molecular Beam Epitaxy (MBE), Chemical Vapor Deposition (CVD) and Metal Organic Vapor Phase Epitaxy (MOVPE) have made it possible to fabricate semiconducting structures with unprecedented precision on the atomic scale in the growth direction, i.e. superlattices, heterojunctions, and quantum wells. The formation of QDs is, on the contrary, largely uncontrolled. In heteroepitaxy the growth starts in a layer by layer mode, giving origin to a wetting layer (WL). This is possible by virtue of the tetragonal deformation of the epilayer, in presence of a coherent strain, up to a certain critical thickness which depends on the materials involved (three to five monolayers for Ge–Si and

* Corresponding author. Tel.: +39-06-55-1771.
E-mail address: motta@fis.uniroma3.it (N. Motta).

0921-5107/03/$ - see front matter © 2003 Published by Elsevier Science B.V.
doi:10.1016/S0921-5107(02)00657-8

1.5–2 ML for InAs/GaAs). Beyond this point, the energy of the system can be lowered by the formation of QDs, governed by a precise energetic law: the increase in the surface energy is compensated by the decrease of the strain allowed by the relaxation of the lattice in the third dimension. Unfortunately the nucleation site, as well as the kinetic formation of a critical nucleus are governed by a number of parameters which are difficult to control. State-of-the-art fabrication techniques require controlled surface patterning as an essential processing step, particularly for wafer scale production. The goal of reducing the dimensions of devices down to the nanometer-scale naturally raises the problem of how to control the patterning of surfaces with a spatial resolution, which is presently not accessible by means of conventional (optical) lithographic techniques. In this context, several studies have shown that long range ordered reconstructions can be used, with varying degrees of success, as templates for the growth of nanostructures [1–3]. Surface nanopatterning has been obtained in various ways, by taking advantage of self-organization (e.g. step bunching on Si surfaces [1] or ripples on misoriented substrates [2,3]), by creating patterns via e-beam lithography [4] or focused ion beams.

In this work we will concentrate on Ge–Si QDs. The interest in these structures has rapidly increased in the last years, because they represent one possible way to create optoelectronic devices directly on Si, which is optically inactive. Another possible application of these structures are highly packed memories for the future computer industry. Due to the 4% lattice mismatch the epitaxial growth of Ge on Si gives origin to nano-islands with dimensions in the range 50–300 nm. The island size is a function of Ge–Si intermixing, which in turn depends on kinetic parameters like the growth temperature, but new growth modes on suitably nanostructured surfaces are expected to shrink the islands dimensions.

Scanning Probe Microscopies (SPM), like Scanning Tunnelling Microscopy (STM) and Atomic Force Microscopy (AFM) [5–9] are the most suited tools to investigate of the structural properties of these structures, and most of the results shown in this paper are obtained thanks to these techniques. But Scanning Probe Microscopes are also used to nanostructure the surface by using voltage pulses to deposit nanoparticles, to create small holes, (acting as nucleation centers of the QD) or to oxidize locally the substrate.

We will start by a brief description of epitaxial growth. In particular the problem of heteroepitaxy, which involves a strain in the epitaxial layer will be addressed. We will describe the different growth modes, as a consequence of increasing lattice mismatch and epitaxial strain. The nucleation and the evolution of coherent islands on flat and nanostructured surfaces will be illustrated in different cases, notably for Ge/Si(111). Self-ordering of islands on stepped surfaces will also be discussed.

2. Ge–Si heteroepitaxy: growth of the wetting layer

The word epitaxy (from the greek words επι (on top) and ταξισ (to order)) indicates a growth mode in which the atoms attach to an existing crystalline surface by forming layers with the same order of the original matrix. We define 'heteroepitaxy' an epitaxial growth realized by depositing an atomic species on a substrate with different composition.

The forces that act between the substrate and the deposited layer give origin to three kinds of growth modes: layer by layer (Frank–Van der Merwe), islands formation on the bare substrate (Volmer–Weber) and a mix of the two: layer by layer up to a critical thickness and island formation above (Stranski–Krastanow). The basic equation that governs the growth mode is the Young–Dupré equation, which can be written as:

$$\gamma_s = \gamma_f \cos\phi + \gamma_{fs} \quad (1)$$

where γ_s is the surface free energy of the substrate and γ_f and γ_{fs} are the surface and interface energies of the film. From a thermodynamic point of view the three growth modes can be derived from the sign of $\Delta\gamma = \gamma_f + \gamma_{fs} - \gamma_s$. In fact, for layer by layer growth, because the surface formation energy γ_s is larger than that of the islands, $\Delta\gamma < 0$ and $\cos\phi = 1$ (this is the case of lattice matched systems; for example, Si on Si). Alternatively, if γ_s is smaller than $\gamma_f + \gamma_{fs}$ this means that $\Delta\gamma > 0$ and for Eq. (1) to hold we must have $\cos\phi < 0$; this means that 3D clusters nucleate on the substrate. This growth mode is typical of large-lattice mismatched systems; for example Ag on GaAs. If $\Delta\gamma$ is negative for the first few monolayers and then changes sign at a critical layer thickness, the growth mode changes from 2D to 3D (Stranski–Krastanow). This one is typical of small-lattice mismatched systems, like for example Ge on Si or InAs/GaAs. Ge/Si could be regarded as a model SK system, because both species belong to the IVth group, their bond being always covalent, without any ionic character. Therefore, the enthalpy at the Ge–Si interface depends essentially on the elastic energy connected to the bond deformation. However, the mixing of the two species is greatly favored (especially at high temperature), and this must be taken into account in the evaluation of the free energy, requiring more complex calculations.

Growth of Ge on Si is a prototype system with small-lattice mismatch, and a WL forms before the nucleation of islands. The way in which this WL evolves is very important to understand the subsequent nucleation of islands. The growth of Ge WL on Si(111) has been followed by STM by several authors [10–13]. At $T =$

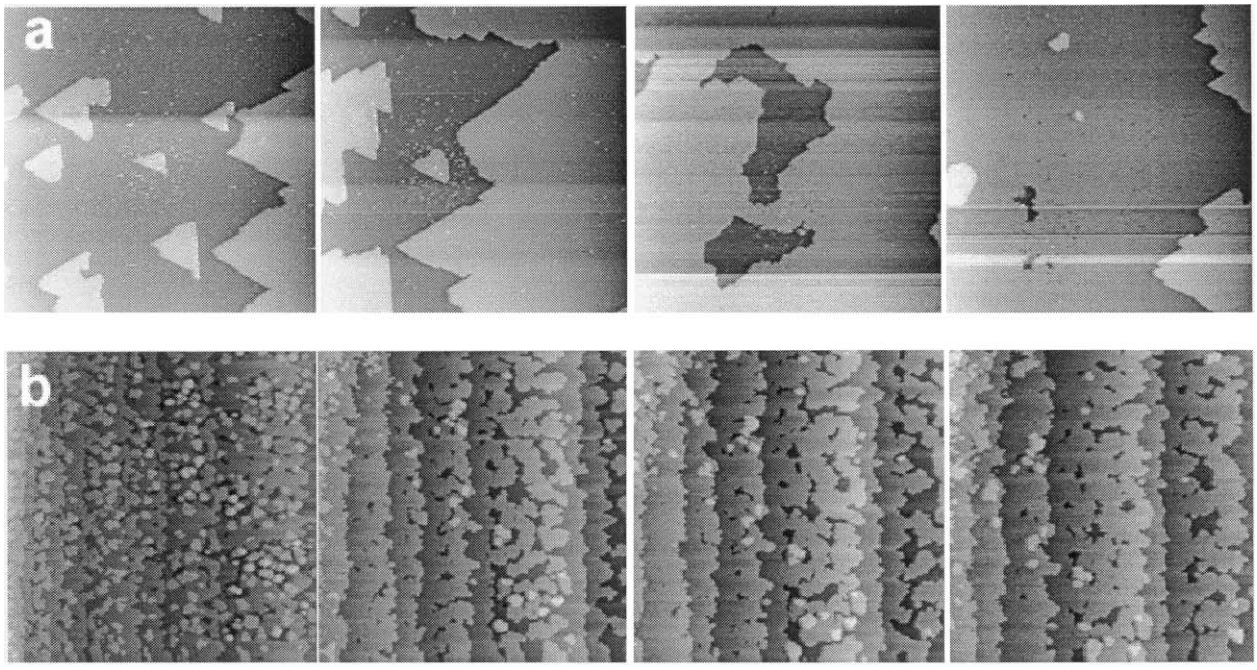

Fig. 1. Ge/Si(111): growth of the WL at $T = 400$ °C. (a) on a step bunched surface with large terraces, low flux (0.02 ML min^{-1}); 0.3×0.3 μm^2 STM images. (b) on a regular surface with small steps, higher flux (0.15 ML min^{-1}), 1×1 μm^2 STM images. Full movies are available at the http://www.fisica.uniroma2.it/infm/nanolab web site.

350 °C and at a deposition rate of a few tenths of monolayers per min we have followed the growth dynamically by STM, taking images of the same area on the surface and arranging them consecutively in a 'movie' (Fig. 1a) showing that the islands nucleate as perfect triangles, and coalesce to give a complete layer [1].

In the movie it is interesting to see that at higher fluxes subsequent layers form, starting from islands of more rounded shapes, with fractal-like borders (Fig. 1b). The evolution of the WL in Ge/Si(111) was discussed recently [10], and it is shown in Fig. 2, starting at 0.65 ML up to 2 ML where the percolation threshold is attained.

The process of coalescence has been modeled by assuming that the clusters are uniformly and randomly distributed over the surface [14,15] and that the nucleation rate of all clusters is δ-like [16]. For triangular islands the dependence of the total perimeter per unit area P of the islands on the fraction of covered surface S is given by:

$$P(S) = \frac{6}{\sqrt[4]{3}} \sqrt{N_o}(1 - S)\sqrt{\ln\frac{1}{1 - S}} \quad (2)$$

where N_o is the number of islands per unit surface. The fit to the distribution of the cluster perimeters extracted from the data of Fig. 2 requires $N_o = 3.8 \times 10^{10}$ islands per cm^2. The order of magnitude of N_o is intermediate between that of metallic clusters on metals [17] and of diamond clusters on semiconductors [18].

It is interesting to investigate the different reconstructions of the surface, changing from 7×7 of bare Si to 5×5 of the complete Ge layer, with mixed areas at intermediate coverages. In the case of Si(111), the 7×7 reconstruction of the clean surface is maintained up to a deposition of 0.45 ML of Ge, as confirmed by the RHEED pattern and by photoelectron diffraction [19,20]. The absence of islands on the terraces and of reconstructed $(2 \times n)$ areas of Ge suggests a process of diffusion of Ge atoms into the Si substrate. As proposed in the case of sub-monolayer deposition of Ge on Si(001), Ge and Si exchange sites [21–23] and the displaced Si diffuses towards the step edges of the substrate (displacive adsorption). Ge 2D islands appearing when Ge coverage exceeds 1 ML, have the typical 5×5 reconstruction [24] with the inclusion of small areas reconstructed 7×7. Such mixed phases disappear at 3 ML coverage, when the surface is flat and fully 5×5 reconstructed, as in Fig. 3.

3. Ge/Si(100): nucleation of coherent islands

Coherent and strained layer by layer growth is favored: for $\varepsilon < \varepsilon_o$ and for $h < h_o$. For $h > h_o$ coherent islands can nucleate. Various models have been suggested to explain the islands' nucleation mechanism [25–37]. Chen and Washburn, following by AFM the formation of Ge/Si(100) coherent islands [38], suggest that 2D platelets grown over the critical size N_c become

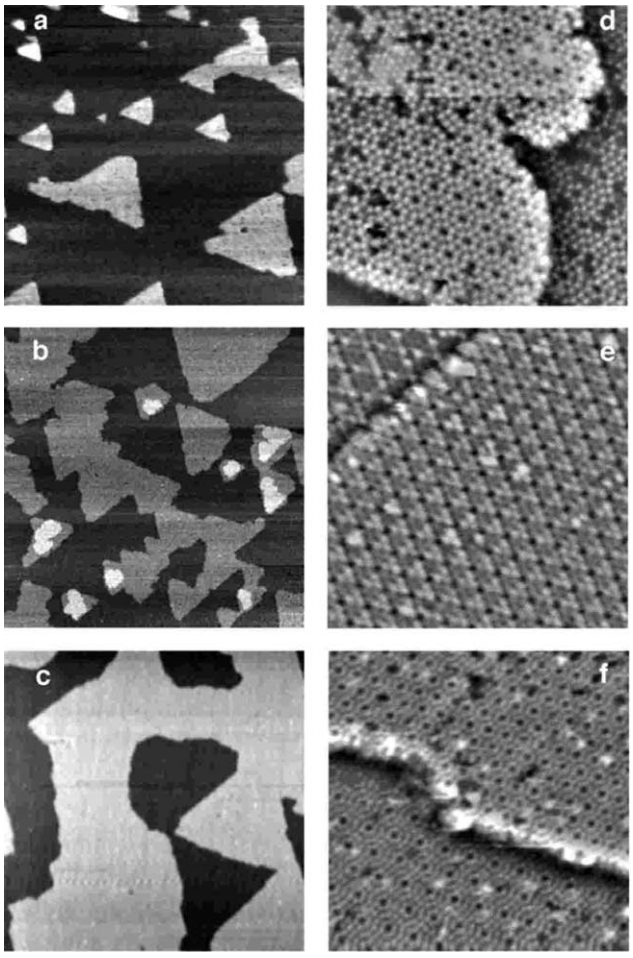

Fig. 2. Left panels: Evolution of the Ge/Si surface (260 × 260) nm^2 for increasing Ge thickness: (a) 0.65 ML; (b) 1.35 ML. (c) 2 ML. Right panels: corresponding zooms (23.5 × 23.5) nm^2 of some island boundaries. Note the $(\sqrt{3}\times\sqrt{3})R30^\circ$ domain in the top left corner of panel (d) and the boundary between the 5×5 and 7×7 reconstructions (in panel (e)). The growth was performed at $T=$ 500 °C with a Ge flux of 0.1 nm min^{-1} [10].

unstable, and the adatoms deposited on the WL tend to diffuse and hop to the top of the platelets. Therefore, 3D islands are formed abruptly, when enough material is available.

The first observation of dislocation-free islands was reported by Eaglesham and Cerullo [39]. They imaged by TEM islands obtained from ~10 nm Ge deposited on Si(001) by MBE at 500 °C. In the same year Mo et al. [40] used STM to unveil the shape and structure of the coherent Ge islands on Si(001). By using physical vapor deposition (PVD) at $T=500$ °C, they obtained elongated 'hut clusters', limited by lateral [501] reconstructed planes, about 10° inclined with respect to the [001] surface. The typical height of these nanocrystals was in the range 2–5 nm, while their base was 20–40 nm. These are the most stable nanostructures of Ge/Si(001) at low coverages. Since the island dimensions decrease by increasing the strain, by using materials like InAs and GaAs it is indeed possible to achieve very small islands. The first to obtain structures under 20 nm were Oshinowo et al. [41] who achieved 15 nm dot size in InGaAs/GaAs. Of course, larger islands can be obtained by a proper choice of the concentration x in the $In_{1-x}Ga_xAs$ alloy. Another parameter controlling the island dimension is intermixing, which always occurs; since it is essentially a kinetic effect, it can be limited by using lower growth temperatures or higher growth rates [42].

3.1. Ge/Si(100): 3D island growth

Very beautiful experiments were carried out by Voigtlaender, who succeeded in taking images of Ge islands grown on Si(001) during nucleation and subsequent stages of growth [43]. STM movies, visible at http://www.fz-juelich.de/video/voigtlaender/ show that

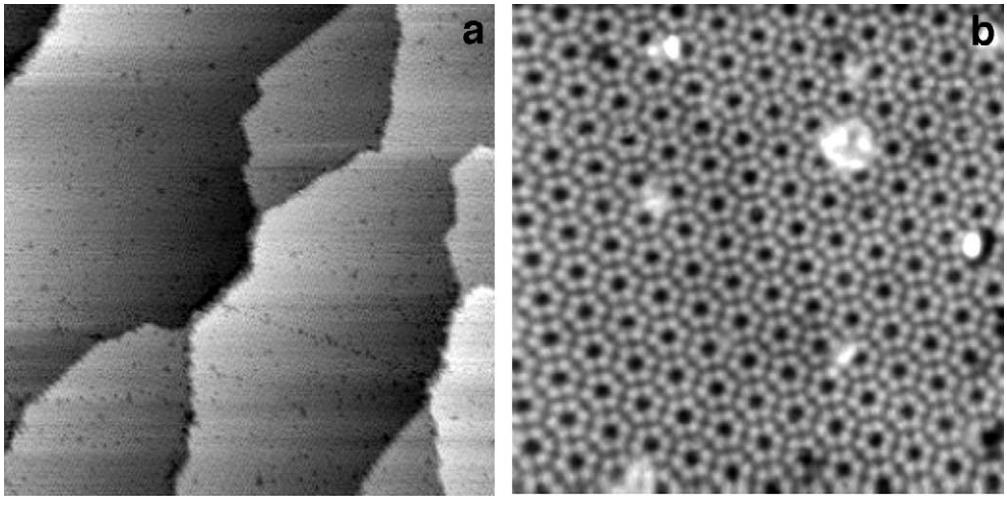

Fig. 3. STM images of Ge/Si(111) WL obtained by 1 nm Ge deposition at 500 °C. (a) 150 × 150 nm; (b) 20 × 20 nm.

Ge islands nucleate as square pyramids, and subsequently one side grows more rapidly than the other, giving origin to the characteristic 'hut' shape.

This growth asymmetry can be described in terms of a slight fluctuation of the growth rate on one face, which completes a plane of atoms faster than the others. The subsequent planes will be also completed faster, because the perpendicular faces are now longer and need more atoms to be filled. This phenomenon is commonly observed at relatively low growth temperatures, in the range 300–500 °C).

Jesson et al. [37] have described the energy change for a square nucleus of side l on the [105] facet of a square based pyramid. The energy needed to grow the layer is positive for small l values, but for large l there is an energy gain due to relaxation, which is higher towards the top of the island. This explains the fact that there are no incomplete atomic planes, because as soon as the square nucleus overcomes the critical value, the rest of the facet is completed very rapidly.

At higher T (>600 °C) Medeiros-Ribeiro et al. [44] have shown that the most stable structure is the square pyramid, along with its evolution (the dome), which appears when enough material is available on the surface. In this context, the islands distribution is fitted with two Boltzmann curves $e^{-\Delta E(n)/KT}$, which represent thermodynamic equilibrium distributions. This means that this kind of Ge islands is stable on Si(001) (whichever of the two shapes is favoured depends only on the number of atoms available). This does not happen on the Si(111) surface. The transition from pyramids to domes can be explained by assuming that there are 2D Ge islands on top of the WL constituting a reservoir. The nanocrystal ensemble can be considered an open system exchanging energy and atoms with 2D islands. The pyramids nucleate and grow up to a maximum volume. At this point the pyramids attract atoms from the 2D islands and the formation of a 'dome' occurs with an abrupt transition. These findings are in agreement with the theoretical predictions of Shchukin et al. [45]. It has been also verified [46] that the island nucleation and evolution is independent from the growth method. Capellini et al. [47–50] and Goryll et al. [51,52] also report on high and low pressure CVD growth of Ge/Si(001) islands, confirming these results, and extending the analysis to dislocated islands. In particular, Goryll et al. [51] analyse Low Pressure CVD Ge/Si(001) samples, grown at $P=0.12$ Torr and $T=525$–700 °C, finding that pyramids are favoured at high deposition rate or small deposition time. Dislocated islands appear beyond a critical height (50 nm).

3.2. Ge/Si(100): 3D island evolution

The evolution of Ge islands after growth during prolonged annealing has been followed by Kamins et al. [46], in order to verify if pyramids and domes are really the most stable structures, or if they are subject to Ostwald ripening, i.e. if the particle size distribution coarsens, driven by the Gibbs–Thomson effect [53]. At high island density Ross et al. [54,55] found that smaller islands shrink during annealing due to evaporation. Kamins et al. [46] also observed a ripening effect which enlarges some of the islands at the expenses of the smaller ones; however, at sufficiently low temperatures the distribution is stable for the two equilibrium shapes: domes and pyramids. Therefore, Kamins et al. state that the coarsening behavior is not consistent with standard Ostwald ripening models [56]. The evolution of Ge islands during Si capping has been followed by STM at very high resolution by Rastelli et al. [57,58]. They find a reversal transition from pyramid to dome with increasing Si coverage. In fact the islands transform into {105} faceted pyramids, and eventually into stepped mounds with steps parallel to the ⟨110⟩ directions. These morphological changes are induced by alloying and represent a complete reversal of those previously observed during Ge island growth. Their results are interpreted with a simple model in which the equilibrium shape of an island mainly depends on its volume and composition.

3.3. Dense arrays of islands

Recently, Springholtz et al. [59] and Floro et al. [60] reported self-organization of Ge–Si islands during growth by MBE. They have shown that generally self-limiting growth does not occur and the system is not equilibrated. Instead, self-organization occurs in a regime of high areal coverage of islands, where short-range repulsive strain interactions between islands drive the organization process. An array of hut clusters self-orders on a square mesh with increasing areal coverage. In case of a dense array of islands, Floro et al. [61] found that ordering occurs to minimize the repulsive elastic interactions between neighbouring islands. However, self-organization breaks down when islands coalesce during deposition or static coarsening.

3.4. Selective growth of 3D Ge islands on patterned Si(001)

Since self-ordering is not easy to obtain, many groups have undertaken alternative routes. One feasible procedure consists in the self assembly of Ge islands on Si(001) patterned substrates.

Kamins et al. [62] have demonstrated dot positioning on Si(001) by using SiO_2 grown on Si(001). They have first realized a local oxidation on the substrate defining Si lines surrounded by oxide. Epitaxial Si(001) is subsequently grown at $T=850$ °C by SiH_2Cl_2 and

HCl, and Ge is deposited from GeH_4 at $T = 600$ °C on this pattern.

A similar procedure was adopted by Vescan et al. [63], in which case the pattern was produced by optical lithography on SiO_2 grown on Si(001). A Si buffer layer (500 nm) is grown at $T = 800$ °C on this patterned substrate, and Ge was subsequently deposited at $T = 700$ °C, 0.3 nm min^{-1} obtaining nice Ge dots aligned at the step edge.

Ishikawa et al. [4] and Kohmoto et al. [65] reported two different approaches for the ordered growth of InAs QDs on GaAs. They first [64] used a combination of in situ electron-beam lithography and Cl_2-gas etching to pattern small and shallow holes on an MBE-grown GaAs(001). When growing more than 1.4 MLs of InAs on the patterned surface, InGaAs dots were observed to preferentially self-organize in the holes while dot formation around the holes was sufficiently suppressed. Their second method [65] is based on a nanometer-scale site-control technique, developed by using STM-assisted nanolithography and self-organizing MBE. Nanometer-scale deposits can be created on a GaAs surface by applying voltage and current pulses by means of an STM tip. These deposits act as nanomasks on which GaAs does not grow directly. Subsequent growth of GaAs thin films yields GaAs nanoholes directly above the deposits. Further deposition of 1.1 ML InAs on this nanostructured surface leads to QDs that are self-organized at hole sites.

Finally, Kim et al. [66] investigated ordering of Ge dot structures by selective epitaxial growth. The dot structures were grown in patterned fine windows ranging in diameter from 650 to 90 nm on Si(100) substrates covered with SiO_2 masks. Dot arrays with excellent size uniformity on the nanometer-scale were reported. The dimensions and number of the dots grown in a window significantly change depending on window size, growth temperature and time and thickness of the Si buffer layer. The dot structures were observed to give rise to prominent luminescence, and the energy position systematically changed when varying growth conditions.

4. Ge/Si(111): formation and evolution of 3D islands

Due to its lesser importance for applications, the Si(111) substrate has been rarely used for Ge growth. However, since 1991 different groups have undertaken the STM study of Ge/Si(111). First of all Kohler et al. [24] visualized the growth of the WL and of the islands on Si(111). It was found that the islands are truncated pyramids, with the top 7×7 or 2×8 reconstructed, depending on the growth temperature.

At Nanolab (University of Rome Tor Vergata) the growth of Ge/Si(111) islands was recently studied in situ. The Si substrate is prepared by flash annealing at 1250 °C through direct current heating, taking care to keep the vacuum level below 5×10^{-10} mbar during the flash. Ge is deposited by PVD from a crucible or using a low-rate e-gun evaporator at a maximum pressure of 2×10^{-10} mbar. Si substrates are kept at 450–550 °C while evaporation rates are typically in the range 0.2–0.5 ML/min (1 ML = 0.314 nm) as determined by a quartz thickness monitor.

3D island nucleation starts at a Ge coverage between 3 and 5 ML, depending on Ge flux and on substrate temperature (Fig. 4), as already noted by Kamins et al. [46]. Typical 3D islands are shown in Fig. 5 where the reconstruction 5×5 of the WL and 7×7 of the top of the islands are visible. Initially islands nucleate as truncated tetrahedra (Fig. 6), with corners pointing in the $\langle 11\bar{2} \rangle$ directions, due to the anisotropy of the growth rate in this direction [24]. The top of the islands is 7×7 reconstructed (Fig. 5b), showing substantial Ge–Si intermixing or at least a modification of the classical Ge(111) reconstruction caused by the stress fields present on the island [67].

Fig. 6b, which displays the gradient of the left image, shows clearly that the island grows irrespectively of substrate stepping, and that the top facet is a [111] plane. The next step in the island evolution is shown in Fig. 7. Now the island is much taller and new steep facets are inserted. This shape transition may be similar to that reported by Medeiros-Ribeiro et al. [44] and Ross et al. [54,55], although in our case the area of the two kinds of islands does not change before and after the insertion of the new facets. Notably, there is a depression (erosion) of the substrate around the island.

The final steps of island evolution are shown in Fig. 8. In panel (a) a gradient image of a Ge island at the first ripening stage is shown. At this stage the shape is rounded, and a large amount of substrate around the island is eroded. The final ripening stage of the island is shown in panel (b); the formation of a central hole (0.6 nm deep) is the most striking feature. The overall process can be qualitatively described as follows: the islands grow vertically up to a critical height, which has been estimated to be about 48 nm [68] after which the strain energy stored inside the islands can be partially relieved by introducing dislocations, or by a morphological transition of the island which progressively becomes more rounded in shape. Concerning the substrate erosion around the island, a similar effect was previously

Fig. 4. Conceptual representation of the formation of Ge islands on Si(111).

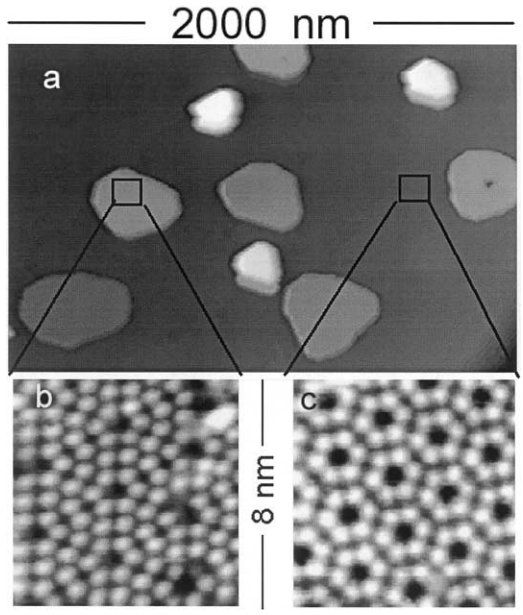

Fig. 5. Topography of a Ge/Si(111) surface after deposition of 9 ML of Ge. (a) STM image 2×1 μm^2. Zooms (8×8) nm^2 (b) on the island's top and (c) on the substrate, displaying the 7×7 reconstruction of the former and the 5×5 of the latter (from [10]).

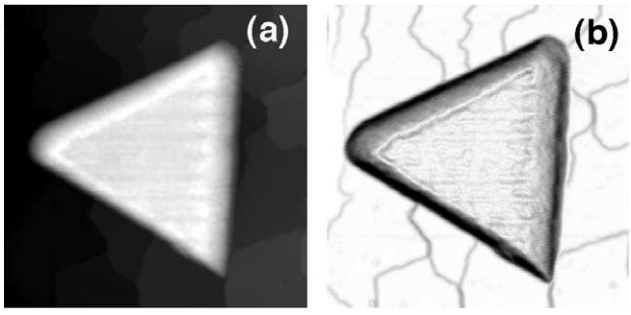

Fig. 6. STM topography of a Ge island deposited on Si(111); $T = 530$ °C, $\theta = 2$ nm; image dimensions are $(236 \times 236 \times 8.5)$ nm^3. (a) Topographic image. (b) Gradient mode image. The gray levels correspond to the angles on the original images (white = 0°; black = 40°).

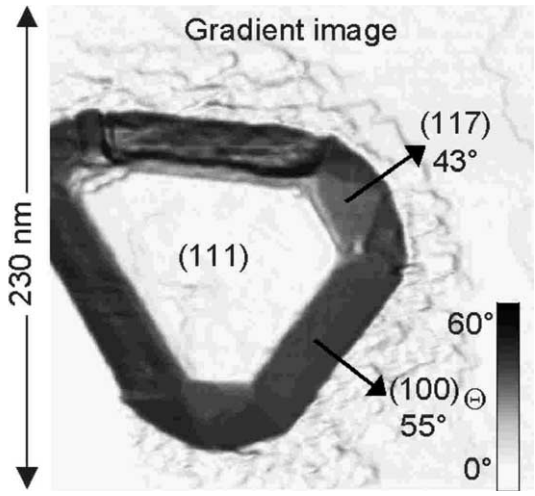

Fig. 7. STM topography, imaged in gradient mode, of a Ge island deposited on Si(111) for $T = 450$ °C and $\theta = 2.5$ nm. Image dimensions are $(230 \times 230 \times 40)$ nm^3. The gray levels correspond to the angles on the original images (white = 0°; black = 60°).

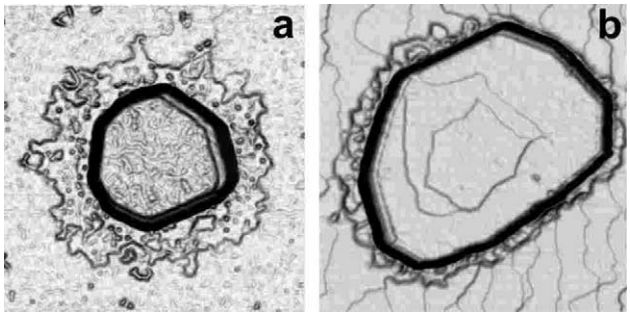

Fig. 8. Ge/Si(111): (a) 527×527 nm^2 STM image in the gradient mode of an island at the first stage of ripening. Island height: 10 nm. (b) 527×527 nm^2 AFM image in the gradient mode of an island transformed in atoll at the final stage. Island height: 8 nm. The two islands belong to different samples grown at $T = 530$ °C (3.5 nm and 2.0 nm of Ge/Si(111), respectively).

reported by Kamins et al. [46] on Ge/Si(100); however, they could not understand clearly its origin due to the oxidation of their samples (the measurements were performed by AFM ex situ, in air) which prevented a clear imaging of the trench.

4.1. Ge–Si: erosion versus intermixing

The results described above lead to the idea that erosion could be assigned to the strong Ge–Si intermixing which draws material from the substrate to create the alloy in the island. With simple geometrical analysis, Liao et al. [69] assume that Si missing from the trenches has gone into alloying within the islands. Seifert et al. [67] have justified the formation of trenches by using a simple model for the local strain energy density: on the WL a compressive area forms around an island, in which the strain energy difference (measured with respect to that of the WL far from the island) is large and positive, while inside the island it is negative [70]. This strain energy gradient is the driving force for the atom current from the WL towards the island [71,72], eroding the substrate that is supposed to be supercritically thick. Subsequently the island experiences a lateral growth, with material flow from the top to the edges; at the same time, the strain propagation along the substrate moves atoms from the WL to the island, eroding the WL itself and the substrate underneath. The driving force coming from the strain can also explain the erosion of the central part in the fully ripened island. In agreement with recent calculations [73,74], we think that

Ge atoms move towards the edge of the island's top facet, where the strain energy can be more efficiently relaxed [71]. Si atoms coming from the substrate in order to relax the strain inside the island lack the mobility [75] necessary to totally replace missing Ge atoms, giving origin to the characteristic 'atoll' shape. Remarkably, the formation of atolls is only observed for Ge grown on Si(111), and has no counterpart on the Si(001) surface.

These data confirm that in semiconductor heteroepitaxy there are four basic mechanisms for strain relief: (a) island nucleation and evolution (shape transition and faceting); (b) formation of dislocations; (c) intermixing and alloying; (d) formation of trenches around the islands. In most cases, a combination of these four mechanisms takes place. We emphasize that the formation of MDs and the occurrence of intermixing can be highly undesired features for the development of applications.

4.2. Self-ordering of Ge islands on Si(111) terraces

It has been shown that during resistive heating of Si(111) a bunching of natural surface steps can form, yielding a simple way to obtain nanostructured Si surfaces. Several authors have studied this phenomenon [76–80], demonstrating that the step configuration at a vicinal surface (with a small misorientation with respect to the (111) plane) during sublimation of a Si crystal depends on the direction of the heating current flowing through the crystal as well as on temperature. The temperature dependence of this effect is not simple, but general agreement exists on the fact that, for Si sublimation at $T > 1220$ °C, step bunching occurs for current flowing in the step-down direction, while a regular step distribution occurs in the step-up direction. In this way we have obtained both regular (i.e. with steps naturally distributed) and step bunched Si(111) surfaces on which we have grown epitaxially Ge at $T =$

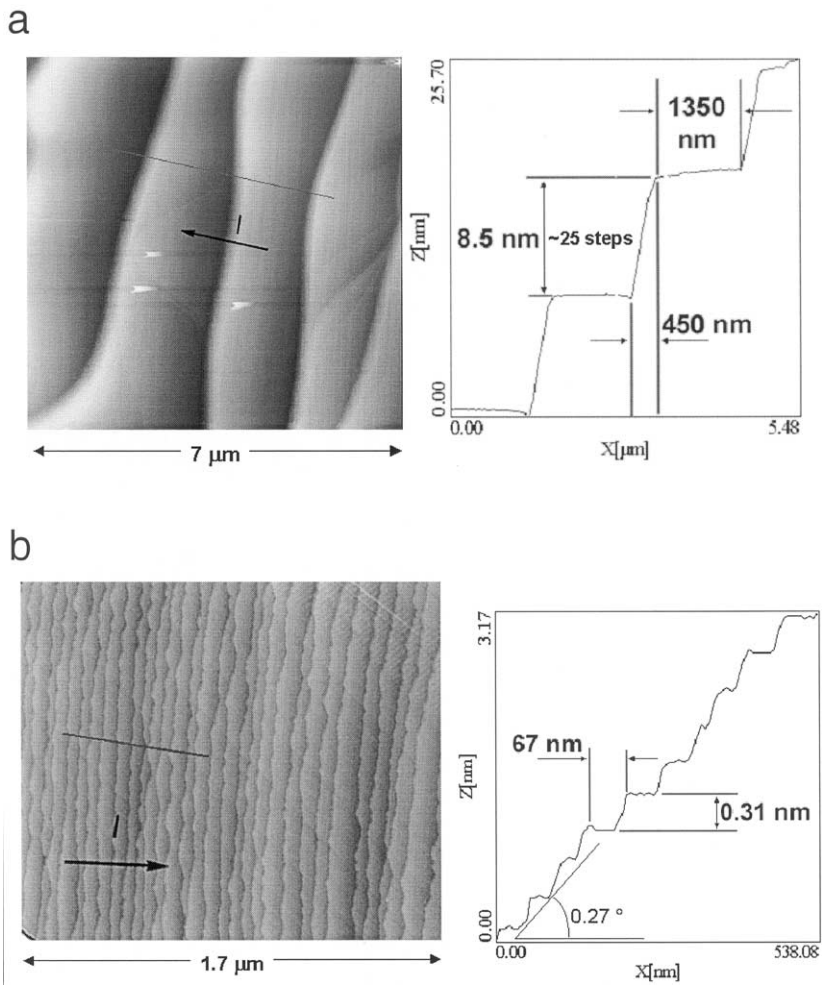

Fig. 9. (a) Left panel: STM topography of a Si(111) surface flashed at $T = 1250$ °C with current flowing in step-down direction; image dimensions are $(7000 \times 7000 \times 36)$ nm^3. Right Panel: Profile taken along the red line. (b) Left Panel: STM topography of a Si(111) surface flashed at $T = 1250$ °C with current flowing in step-up direction; image dimensions are $(1700 \times 1700 \times 10)$ nm^3. Right Panel: Profile taken along the red line.

450 and 530 °C. (Fig. 9) We have analyzed by STM and AFM the evolution and distribution of the islands on different surfaces. An evident self-ordering on step bunched surfaces exists and the parameters of this ordering were studied.

By keeping the annealing temperature in the range 1220–1250 °C, and applying the voltage in the step-down direction [1], the surface reorganizes forming large terraces (width >1 μm) separated by groups of small steps (width ≈ 10 nm). In this case the islands start nucleating and evolving on the step borders due to the Schwoebel effect: the atoms coming from the terrace are reflected at the lower step edge, but are incorporated in the upper step. On terraces nucleation takes place only when step decoration is nearly completed. For 2.5 nm coverage (Fig. 10a) a line of equally spaced islands appear at the center of the terraces, while borders are decorated by ribbons of ripened islands. They have a regular distribution, with a mean spacing of 0.36 μm and a mean distance from the steps of 0.62 μm. The mean spacing gives a rough estimate of the diffusion length of Ge on these surfaces. At 6 nm (Fig. 10b) several generations of islands are present on terraces, from the youngest (tall and triangular) to the oldest (rounded, atoll-like), while step edges are covered by a continuous ribbon. As previoulsy discussed, regular distribution of islands can been obtained by CVD growth on patterned Si(100) [62–66]. Our experiments show that in principle the same is possible on Si(111) just by using the natural patterning due to step bunching.

By applying the voltage in the step-up direction during annealing at $T = 1220$ °C steps distribute uniformly (step width ≈ 70 nm). On this regular substrate islands nucleate without any specific ordering (Fig. 10 c–d) except for a tendency of the islands to align in the direction parallel to the step borders. It is also noteworthy that tetrahedral islands point in the same $\langle 11\bar{2} \rangle$ direction both on step bunched and on regular surfaces.

4.3. Ge/Si(111): effects of sample annealing

In order to analyse the effect of annealing on Ge islands, we have grown two different samples at 500 °C by depositing 4 nm Ge on Si(111) at 0.05 nm min^{-1} [68]. The two samples were annealed at 500 °C just after growth for 5 and 30 min.

In Fig. 11a we report the height distribution of the island sizes of the above-mentioned samples obtained performing measurements on about 200 islands. In the curve of the 5 min annealed sample we recognize a peak (A) centered around 48 nm and a broad structure (B) centered around 20 nm. In the 30 min annealed sample we observe a narrowing of the B band to just one peak, and a shift of structures A and B toward lower height. This means that the islands are not stable against annealing, and there is a tendency to relax the stress by moving atoms from the island top to the base. The

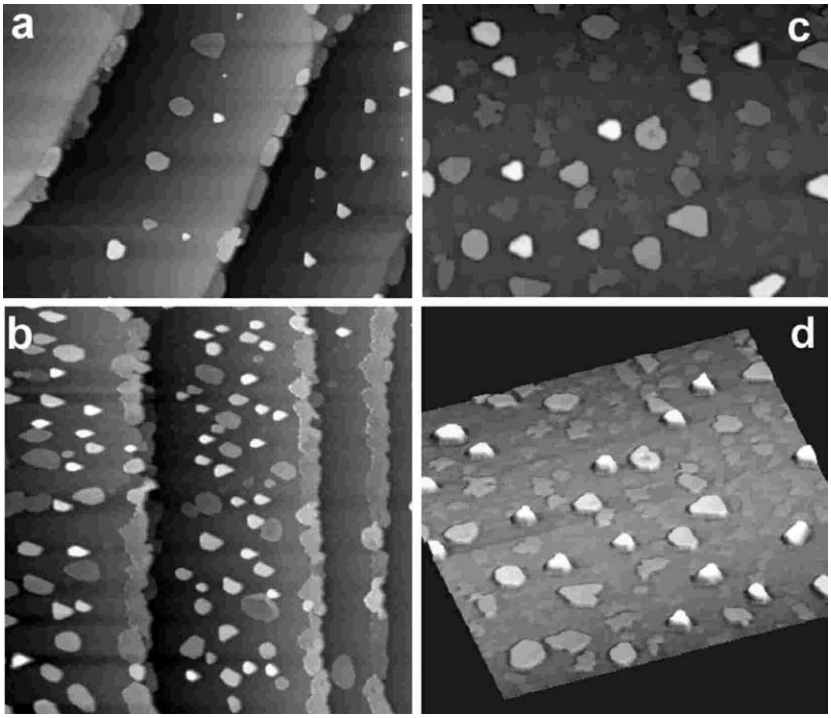

Fig. 10. (a) STM image of 2.5 nm Ge deposition on Si(111) at $T = 450$ °C 2.7×2.7 μm^2. The total height of the image is 56 nm. (b) STM image of 6 nm Ge deposition on Si(111) at $T = 450$ °C 10×10 μm^2. The total height of the image is 82 nm. (c) 5.4 nm Ge deposited at $T = 500$ °C on a regular surface: (3×3) μm^2; vertical scale: 29 nm. (d) 3D representation of image (c). The Si(111) substrate has been flashed at $T = 1200$ °C.

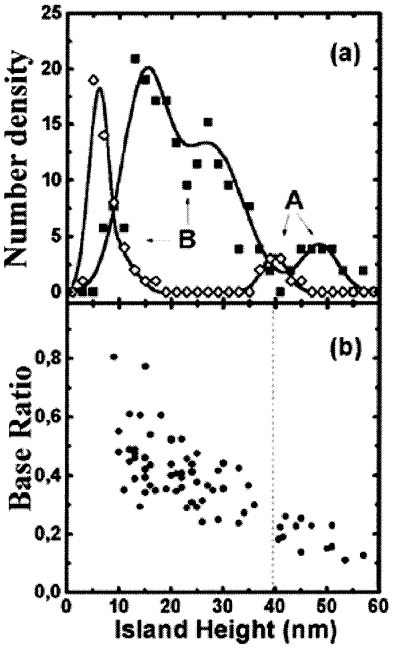

Fig. 11. (a) Island height distribution of the 5 min (square) and 30 min annealed (diamond) sample. (b) Ratio R between the top and bottom base size of the islands in the 5 min annealed sample. The vertical dashed line separates A-type from B-type islands. From [68].

introduction of MD surely plays a role in this transition, by changing the island shape from truncated tetrahedra to flat disks, up to the last stage of atolls.

Comparing the effects seen during annealing with those observed during growth we are able to discuss the evolution of 3D islands. By increasing Ge coverage, the islands grow via a SK self-assembling mechanism as truncated tetrahedra until they reach a height of about 48–50 nm. In agreement with the case of Ge/Si(100) [47,48], we take this value as the critical height for the introduction of MDs. In fact it has been reported that when the strain energy stored in the island is too high, MDs are inserted in the [110] direction [81].

The regions where a MD has been inserted are stress free and thus are preferential sites for Ge attachment [47,48,70]. In our case we suggest that this mechanism drives the morphological evolution of the islands from coherent to dislocated during annealing. During the annealing procedure we can observe the evolution of this relaxation in time, keeping fixed the amount of Ge atoms deposited. As during growth, the atoms that are bound on the top of a strained island experience a stress that decreases the energy barrier for detachment [82]. On the contrary, the sites a dislocation has been inserted have a higher binding energy: this difference on the energy gained by the system bonding an atom (i.e. an inhomogeneous chemical potential) generates a flow of atoms [83] that depletes the top of the island and increases the material deposited at its base. In this way we can have a damping of the island that increases the dimension of the top facet and decreases the contact angle of the facets, in agreement with our observations.

5. Conclusions

We have shown how SPM techniques can provide valuable insight on the growth and morphology of semiconductor QDs. We have analysed the origin of QD formation, which is connected to the strain arising from the difference in the lattice parameters between substrate and epilayer. At a critical layer thickness, the growth mode changes from 2D to 3D and small islands appear. We have analysed in detail the growth of QDs in a model system: Ge/Si. This could be regarded as a typical SK system, but intermixing between Ge and Si is very important especially at high temperatures, often limiting the minimum dot size to more than 100 nm. We have analysed firstly the evolution and the composition of the WL and then the nucleation and the formation of coherent 3D islands. On Si(100) substrates, QDs nucleate as square based pyramids, evolving into domes which are the most stable structures. Dislocated islands appear beyond a certain size, if Ge deposition is continued. The final island evolution depends on the subsequent thermal treatment, and eventually dislocated and ripened islands appear. On Si(111) substrates islands are observed to nucleate as truncated tetrahedra, adding new facets as their size increase. Since Si(111) is a minimum energy surface, the islands tend to flatten and to enlarge the top (111) face. Many dislocations are introduced, and the final shape resembles an ‘atoll’ due to the erosion of the central part of the island. This erosion is believed to be caused by a tensile stress found by the atoms in this region, due to the particular composition profile.

We have discussed issues related to stability and the possible routes to grow ordered arrays of QDs, notably self-ordering caused by repulsive strain fields on Si(001), lithographic positioning and selective epitaxial growth on Si(001), or by step bunched surfaces on Si(111).

The possible applications of Ge/Si QDs are various, but only the creation of nanomemories actually seems to be a viable option. There is still a lot of work to be carried out in this field, in order to find a suitable way for generating ordered arrays of perfect QD structures. Many solutions have been suggested combining standard lithography and self-assembly (see for example Omi et al. [84]). Also the problem of connecting these structures has not yet been solved. It is actually not known if the miniaturization of future electronics will be reached by self assembled QDs, producing nanoelectronic devices, i.e. if these structures can be really grown in an organized way and with the desired shape and size.

Acknowledgements

This work was partially supported by EEC (FORUM-FIB IST-2000-29573 contract) and by INFM. We are grateful to Dr R. Calarco and to Dr G. Capellini for collaborating on some STM and AFM results.

References

[1] N. Motta, A. Sgarlata, F. Rosei, A. Balzarotti, Mater. Res. Symp. Proc. 696 (2002) N2.2.1.
[2] J. Zhu, K. Brunner, G. Abstreiter, Appl. Phys. Lett. 73 (1998) 620.
[3] (a) I. Berbezier, A. Ronda, A. Portavoce, J. Phys. Cond. Matter, 14 (2002) 8283.
[4] T. Ishikawa, S. Kohmoto, K. Asakawa, Appl. Phys. Lett. 73 (1998) 1712.
[5] G. Binnig, H. Rohrer, Rev. Mod. Phys. 71 (1999) S324.
[6] J.A. Kubby, J.J. Boland, Surf. Sci. Rep. 26 (1996) 61.
[7] R.J. Hamers, Ann. Rev. Phys. Chem. 40 (1989) 531.
[8] B. Voigtlaender, A. Zinner, Appl. Phys. Lett. 63 (1993) 3055.
[9] B. Voigtländer, Surf. Sci. Rep. 43 (2001) 127.
[10] N. Motta, A. Sgarlata, R. Calarco, Q. Nguyen, F. Patella, J. Castro Cal, A. Balzarotti, M. De Crescenzi, Surf. Sci. 406 (1998) 254.
[11] F. Arciprete, A. Balzarotti, M. Fanfoni, N. Motta, F. Patella, A. Sgarlata, Recent Res. Dev. Vacuum Sci. Tech. 3 (2001) 71.
[12] T. Fukuda, Surf. Sci. 351 (1996) 103.
[13] F. Rosei, N. Motta, A. Sgarlata, A. Balzarotti, Lecture Notes Phys. 588 (2002) 252.
[14] M. Avrami, J. Chem. Phys. 7 (1939) 1103.
[15] M. Avrami, J. Chem. Phys. 8 (1940) 212.
[16] M. Tomellini, M. Fanfoni, Surf. Sci. 349 (1996) L191.
[17] H. Brune, H. Roder, C. Boragno, K. Kern, Phys. Rev. Lett. 73 (1994) 1955.
[18] R. Polini, M. Tomellini, M. Fanfoni, F. Le Normand, Surf. Sci. 373 (1997) 230.
[19] M.A. Lamin, O.P. Pchelyakov, L.V. Sokolov, S.I. Stenin, A.I. Toropov, Surf. Sci. 207 (1989) 418.
[20] M. De Crescenzi, R. Gunnella, R. Bernardini, M. De Marco, I. Davoli, Phys. Rev. B 52 (1995) 1806.
[21] R.M. Tromp, Phys. Rev. B 47 (1993) 7125.
[22] L. Patthey, E.L. Bullock, T. Abukawa, S. Kono, L.S.O. Johansson, Phys. Rev. Lett. 75 (1995) 2538.
[23] K.H. Huang, T.S. Ku, D.S. Lin, Phys. Rev. B 56 (1997) 4878.
[24] U. Köhler, O. Jusko, G. Pietsch, B. Muller, M. Henzler, Surf. Sci. 248 (1991) 321.
[25] R.M. Feenstra, J.A. Stroscio, J. Tersoff, A.P. Fein, Phys. Rev. 58 (1987) 192.
[26] R.M. Feenstra, Phys. Rev. Lett. 63 (1989) 1412.
[27] H.W.M. Salemink, O. Albrektsen, Phys. Rev. B 47 (1993) 16044.
[28] R.S. Becker, J.A. Golovchenko, B.S. Swartzentruber, Phys. Rev. B 32 (1985) 8455.
[29] X.R. Qin, B.S. Swartzentruber, M.G. Lagally, Phys. Rev. Lett. 84 (2000) 4645.
[30] P. Sutter, M.G. Lagally, Phys. Rev. Lett. 84 (2000) 4637.
[31] P.W. Deelman, T. Thundat, L.J. Schowalter, Appl. Surf. Sci. 104/105 (1996) 510.
[32] F. Liu, M.G. Lagally, Phys. Rev. Lett. 76 (1996) 3156.
[33] F. Liu, M.G. Lagally, Chem. Rev. 97 (1997) 1045.
[34] P.C. Kelires, J. Tersoff, Phys. Rev. Lett. 63 (1989) 1166.
[35] D.E. Jesson, S.J. Pennycook, J.M. Baribeau, Phys. Rev. Lett. 66 (1991) 750.
[36] D.E. Jesson, M.F. Chrisholm, S.J. Pennycook, J.M. Baribeau, Phys. Rev. Lett. 75 (1995) 184.
[37] D.E. Jesson, K.M. Chen, S.J. Pennycook, MRS Bull. 21 (n. 4) (1996) 31.
[38] Y. Chen, J. Washburn, Phys. Rev. Lett. 77 (1996) 4046.
[39] D.J. Eaglesham, M. Cerullo, Phys. Rev. Lett. 64 (1990) 1943.
[40] Y.-W. Mo, D.E. Savage, B.S. Swartzentruber, M.G. Lagally, Phys. Rev. Lett. 65 (1990) 1020.
[41] H. Oshinowo, M. Nishioka, S. Ishida, Y. Arakawa, Appl. Phys. Lett. 65 (1994) 1422.
[42] F. Patella, M. Fanfoni, F. Arciprete, S. Nufris, E. Placidi, A. Balzarotti, Appl. Phys. Lett. 78 (2001) 320.
[43] M. Kastner, B. Voigtlaender, Phys. Rev. Lett. 82 (1999) 2745.
[44] G. Medeiros-Ribeiro, A.M. Bratkovski, T.I. Kamins, D.A. Ohlberg, R. Stanley Williams, Science 279 (1998) 353.
[45] V.A. Shchukin, N.N. Ledentsov, P.S. Kopev, D. Bimberg, Phys. Rev. Lett. 75 (1995) 2968.
[46] T.I. Kamins, G. Medeiros-Ribeiro, D.A.A. Ohlberg, R. Stanley Williams, J. Appl. Phys. 85 (1999) 1159.
[47] G. Capellini, L. Di Gaspare, F. Evangelisti, E. Palange, Appl. Phys. Lett. 70 (1997) 493.
[48] G. Capellini, L. Di Gaspare, F. Evangelisti, E. Palange, Semicond. Sci. Technol. 14 (1999) L21.
[49] E. Palange, G. Capellini, L. Di Gaspare, F. Evangelisti, Appl. Phys. Lett. 68 (1996) 2982.
[50] E. Palange, L. Ragni, L. Di Gaspare, G. Capellini, F. Evangelisti, J. Appl. Phys. 83 (1998) 5840.
[51] M. Goryll, L. Vescan, K. Schmidt, S. Mesters, H. Luth, K. Szot, Appl. Phys. Lett. 71 (1997) 410.
[52] M. Goryll, L. Vescan, K. Schmidt, S. Mesters, H. Luth, K. Szot, Mater. Sci. Eng. B69–70 (2000) 251.
[53] W. Ostwald, Z. Phys. Chem. 34 (1900) 495.
[54] F.M. Ross, R.M. Tromp, M.C. Reuter, Science 286 (1999) 193.
[55] F.M. Ross, J. Tersoff, R.M. Tromp, Phys. Rev. Lett. 80 (1998) 984.
[56] M. Zinke-Allmang, L.C. Feldman, M.H. Grabow, Surf. Sci. Rep. 16 (1992) 377.
[57] A. Rastelli, M. Kummer, H. von Kanel, Phys. Rev. Lett. 87 (2001) 256101.
[58] A. Rastelli, E. Muller, H. von Kanel, Appl. Phys. Lett. 80 (2002) 1438.
[59] G. Springholz, V. Holy, M. Pinczolits, G. Bauer, Science 282 (1998) 734.
[60] J.A. Floro, E. Chason, M.B. Sinclair, L.B. Freund, G.A. Lucadamo, Appl. Phys. Lett. 73 (1998) 951.
[61] J.A. Floro, M.B. Sinclair, E. Chason, L.B. Freund, R.D. Twesten, R.Q. Hwang, G.A. Lucadamo, Phys. Rev. Lett. 84 (2000) 701.
[62] T.I. Kamins, R. Stanley Williams, Appl. Phys. Lett. 71 (1997) 1201.
[63] L. Vescan, K. Grimm, M. Goryll, B. Hollander, Mater. Sci. Eng. B69 (2000) 324.
[64] T. Ishikawa, S. Kohmoto, K. Asakawa, Appl. Phys. Lett. 73 (1998) 1712.
[65] S. Kohmoto, H. Nakamura, T. Ishikawa, K. Asakawa, Appl. Phys. Lett. 75 (1999) 3488.
[66] E.S. Kim, N. Usami, Y. Shiraki, Semicond. Sci. Technol. 14 (1999) 257.
[67] W. Seifert, N. Carlsson, J. Johansson, M. Pistol, L. Samuelson, J. Cryst. Growth 170 (1977) 39.
[68] G. Capellini, N. Motta, A. Sgarlata, R. Calarco, Solid State Comm. 112 (1999) 145.
[69] X.Z. Liao, J. Zou, D.J.H. Cockayne, Z.M. Jiang, X. Wang, R. Leon, Appl. Phys. Lett. 77 (2000) 1304.
[70] F.K. Le Goues, M.C. Reuter, J. Tersoff, M. Hammar, R.M. Tromp, Phys. Rev. Lett. 73 (1994) 300.
[71] A.L. Barabási, Appl. Phys. Lett. 70 (1997) 2565.

[72] S.A. Chaparro, Y. Zhang, J. Drucker, Appl. Phys. Lett. 76 (2000) 3534.
[73] J. Tersoff, Phys. Rev. Lett. 81 (1998) 3183.
[74] B.J. Spencer, J. Tersoff, Phys. Rev. B 63 (2001) 205424.
[75] J. Tersoff, Phys. Rev. Lett. 85 (2000) 2843.
[76] J.J. Metois, S. Stoyanov, Surf. Sci. 440 (1999) 407.
[77] Y. Homma, N. Aizawa, Phys. Rev. B 62 (2000) 8323.
[78] H.-C. Jeong, E.D. Williams, Surf. Sci. Rep. 34 (1999) 171.
[79] K. Yagi, H. Minoda, M. Degawa, Surf. Sci. Rep. 43 (2001) 45.
[80] F.K. Men, F. Liu, P.J. Wang, C.H. Chen, D.L. Cheng, J.L. Lin, F.J. Himpsel, Phys. Rev. Lett. 88 (2002) 096105.
[81] F.K. Le Goues, M.C. Reuter, M. Hammar, R.M. Tromp, Surf. Sci. 349 (1996) 249.
[82] H.T. Dobbs, D.D. Vvedensky, A. Zangwill, J. Johansson, N. Carlsson, W. Seifert, Phys. Rev. Lett. 79 (1997) 897.
[83] M. De Crescenzi, R. Gunnella, R. Bernardini, M. De Marco, I. Davoli, Phys. Rev. B 52 (1995) 1806.
[84] H.S. Omi, D.S. Bottomley, T.J. Ogino, Appl. Phys. Lett. 80 (2002) 1073.